JOURNAL OF COMPUTATIONAL PHYSICS 56, 428–447 (1984)

An Efficient Computation Scheme for Tracking Contaminant Concentrations in Fluid Flows*

J. M. SICILIAN AND C. W. HIRT

Flow Science, Inc., 1325 Trinity Drive, Los Alamos, New Mexico 87544

Received May 4, 1983; revised November 8, 1983

It is often important in engineering applications to predict the concentration of contaminants in a fluid flow. The prediction of the time-dependent behavior of contaminant concentrations in three dimensions is usually expensive, particularly when the arrival time of concentration fronts is important. An efficient numerical solution algorithm for such problems based on the use of discrete fluid particles to represent the contaminants, and a continuum representation of the background fluid is discussed. The Containment Atmosphere Prediction (CAP) code has been developed to apply this scheme to the analysis of hydrogen distribution in nuclear reactor containment buildings under postulated degraded-core accident conditions. CAP is described and comparisons between its predictions and experimental results presented.

I. INTRODUCTION

Among the useful (and sometimes annoying) properties of fluid flows is their ability to transport contaminants. Important examples in engineering practice include: transport of pollutants in the atmosphere; ground water and surface water dispersion; flow of neutron-absorbing poisons through nuclear-reactor coolant systems; mixing of hydrogen and steam with air in nuclear-reactor containment buildings under postulated degraded-core accident conditions; transport of chemical species in reacting process systems; and mixing of materials in various casting methods.

The influence of the contaminants on the overall flow varies greatly among these examples. In some cases the contaminant simply flows with the fluid, making minor modifications to the fluid properties (i.e., viscosity, density). Other contaminants move relative to the mean fluid as well as being transported with it and affect the fluid properties more strongly. This relative motion can introduce interesting effects when the contaminant modifies the fluid properties as well. In this case the mean fluid motion may be distorted or even dominated by the location and properties of the contaminant.

Numerical simulations of contaminant flows have previously used a variety of modeling techniques. Flows in which the contaminant moves passively with the flow

* Work supported under EPRI/NSAC Contract TSA82-521.

0021-9991/84 $3.00

can often be addressed by standard methods. The SOLA-3D code [1, 2], for example, treats contaminants in three-dimensional, incompressible flows by tracing the motion of contaminant marker particles. These particles have, however, no influence on the flow itself.

The PIC[3] method used fluid particles to represent all mass in the flow, both contaminants and the background atmosphere. This method does represent the influence of contaminants on the flow, and with appropriate modifications can represent relative motion as well.

Another class of solution techniques is based on the multiphase/multifluid flow equations. Several programs [4–6] have been developed for the analysis of transients in nuclear reactors involving the flow of two-phase fluids. These methods represent two (or more) fluids as continuum functions on a computational mesh. The continuum equations for the coupled fluid flows, which include models for mass, momentum, and energy exchange between the phases, are then solved numerically.

In this paper we propose a union of the particle and continuum viewpoints, designed specifically for the solution of contaminant flow problems. The algorithm is developed in the hope of providing a more efficient tool for numerical simulation of such flows. The contaminants are represented by discrete fluid particles in this method, while the flow environment is represented as a continuum on an Eulerian grid. The influence of the contaminants on the fluid motion is easily accounted for in this algorithm by integrating the influence of individual particles over each Eulerian mesh cell.

We anticipate increased efficiency for this union because a relatively coarse mesh may be used for the continuum, while reasonable numbers of particles represent the contaminants. A coarse mesh may be used because numerical diffusion of the contaminant is eliminated by the use of the Lagrangian-like particles. Of course, overall accuracy is limited by the complexity of the flow patterns which evolve in the physical situation. Unless these are adequately resolved by the computational grid, the benefits of the particle representation are limited. In many cases, however, the mean flow is quite smooth and the effects of turbulence can often be treated by auxiliary models not requiring detailed mesh resolution. Small numbers of particles may be used when the contaminants constitute a small proportion of the fluid material. As the contaminant concentration increases, more particles may be required to provide a more continuous representation of the contaminant (i.e., one which keeps fluctuations associated with the particles to an acceptably low level).

The Containment Atmosphere Prediction (CAP) code has been developed employing this algorithm to investigate the mixing of hydrogen, steam, and air in nuclear-reactor containment buildings. The CAP program provides the specific example through which we describe the use of the method. Therefore, several aspects of the hydrogen transport and mixing problem require discussion.

Interest in the mixing of hydrogen in nuclear-reactor containment buildings has renewed because of the combustion of hydrogen during the Three Mile Island accident [7]. Hydrogen is produced in nuclear reactors by the radiolysis of water and, under postulated degraded-core accident conditions, by the reaction of fuel-rod

cladding (Zircaloy) with coolant water. During a degraded-core accident, such as occurred at Three Mile Island, large amounts of hydrogen can be produced. If vented to the containment atmosphere, this hydrogen has the potential of burning and may threaten containment integrity or affect the operability of essential safety equipment. In the event of containment failure, radioactive material may be released to the environment. As a result of the Three Mile Island accident, the U.S. Nuclear Regulatory Commission has required the installation of hydrogen control systems in various nuclear reactor containments to control hydrogen generated in a postulated degraded-core accident and thereby assure containment integrity [8]. Previous investigations of hydrogen mixing have used derivatives of multiphase/multifluid programs [9–11].

All of the effects that are important to this problem are included in the CAP code. Steam and hydrogen mass are represented by particles flowing in an atmosphere of air. They diffuse in response to concentration gradients and influence the net atmospheric density. The three-dimensional continuum equations used for the atmosphere flow are the compressible-flow conservation equations for mass, momentum, and energy.

Sources and sinks of steam, hydrogen, air, energy, and momentum are provided. Because the desire for large mesh cells conflicts with the complexity of geometry, a capability for partial blockage of cell faces and volumes has been incorporated into the CAP program. Similarly, contaminant concentration detectors, whose resolution is independent of mesh cell size, are available to indicate local concentration histories.

The following sections of this paper present the equations solved by CAP, the solution algorithm (with emphasis on the union of particle and continuum representations), and comparisons of code predictions with experiments and with analytic solutions.

II. Continuum Equation Formulation and Difference Approximations

The equations for flow of a contaminant in a surrounding atmosphere are separated for this algorithm into continuum and discrete (particle) components. The discrete component determines the location and mass of the contaminant, while the continuum equations specify the mixture flow field (velocity) and energy distribution, and the atmospheric (air) density. The atmosphere is assumed to behave as a mixture of perfect gases at the same temperature. The continuum equations solved are the conservation of momentum and internal energy for the mixture and the conservation of air mass. (Conservation of hydrogen and steam masses are ensured by the particle representation.) In vector notation these conservation equations are

$$\text{Mass:} \qquad \frac{\partial \rho_a}{\partial t} + \bar{\nabla} \cdot \rho_a \bar{u} = S_\alpha / \text{Vol} \tag{1}$$

$$\text{Momentum:} \qquad \rho \frac{\partial \bar{u}}{\partial t} + \rho(\bar{u} \cdot \bar{\nabla})\bar{u} = -\bar{\nabla}p + \rho\bar{g} + (\bar{S}_m - \bar{u}S_a)/\text{Vol} \tag{2}$$

$$\text{Internal Energy:} \qquad \frac{\partial \rho I}{\partial t} + \bar{\nabla} \cdot (\rho I \bar{u}) = -p\bar{\nabla} \cdot \bar{u} + S_e/\text{Vol} \tag{3}$$

where

ρ_a is the air macroscopic density
ρ is the total (air + hydrogen + steam) macroscopic density
$\bar{u}$ is the mixture velocity
p is the mixture pressure
$\bar{g}$ is the gravitational acceleration
I is the mixture specific internal energy

and S_a, $\bar{S}_m$, and S_e are external sources of air mass, mixture momentum and mixture energy, respectively.

For simplicity, we have not represented the blockage of flow area or volume in these continuum equations. Blockages are introduced in the finite-difference formulation.

Solution of Eqs. (1)–(3) produces the air density, the mixture velocity field, and the mixture internal energy field. As described in Section III, the particle transport solution provides the densities of hydrogen and steam. It is assumed in CAP that all components have the same velocity, that is, there is no slip. Condensation of steam is treated in the particle domain. Since liquid water is not considered by CAP, condensation produces only a source term in the mixture energy equation (and, of course, a sink of mixture mass).

Equations (1)–(3) are solved by finite-difference methods on a staggered three-dimensional mesh. The mesh structure and finite-difference formulations are essentially those of the SOLA-3D program [2]. (Although the CAP code operates in either Cartesian or cylindrical coordinates, in this paper we will present only the Cartesian representation.) Each mesh cell is identified by an ordered triplet (i, j, k) where i is the x-cell index, j is the y-cell index, and k is the z-cell index. Pressure, density, and internal energy are evaluated at cell centers and velocities on cell faces. Figure 1 shows the locations of the three velocity components for cell (i, j, k). The velocity in the x direction is called u; in the y direction, v; and in the z direction, w. These locations imply solution of the three components of the momentum equation on staggered cells.

The calculation proceeds as a sequence of forward time steps. The time level of a variable is indicated by a single superscript. Thus, the pressure at the center of cell (3, 4, 5) after 10 time steps is indicated by $P^{10}_{3,4,5}$.

With these definitions the finite-difference forms of the continuum equations solved are:

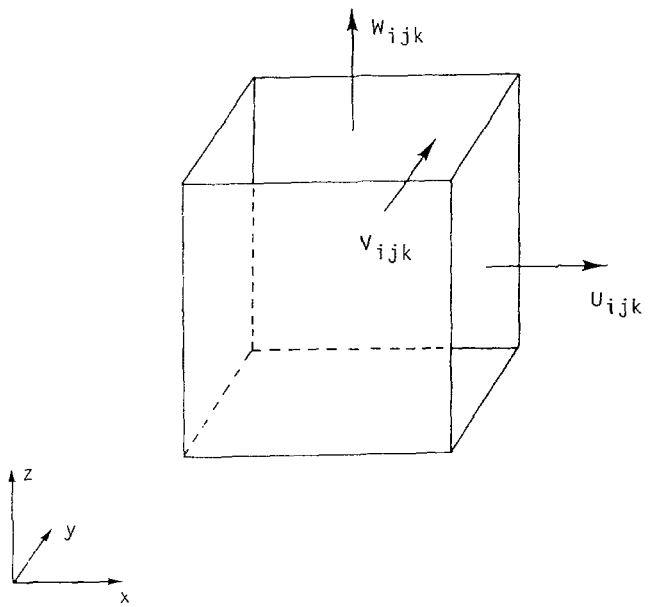

FIG. 1. Mesh cell with velocity locations.

Air mass conservation

$$\frac{\rho_{a_{i,j,k}}^{n+1}-\rho_{a_{i,j,k}}^{n}}{\delta t^{n+1}}=\frac{1}{\mathrm{VOL}_{i,j,k}}\left[S_{a_{i,j,k}}^{n+1}-\mathrm{FRAX}_{i,j,k}^{n}+\mathrm{FRAX}_{i-1,j,k}^{n}\right.$$
$$\left.-\mathrm{FRAY}_{i,j,k}^{n}+\mathrm{FRAY}_{i,j-1,k}^{n}-\mathrm{FRAZ}_{i,j,k}^{n}+\mathrm{FRAZ}_{i,j,k-1}^{n}\right] \quad (4)$$

X-component mixture momentum equations

$$\frac{u_{i,j,k}^{n+1}-u_{i,j,k}^{n}}{\delta t^{n+1}}=S_{v_{i,j,k}}^{x^{n+1}}-\frac{P_{i+1,j,k}^{n+1}-P_{i,j,k}^{n+1}}{\frac{1}{2}(\rho_{i,j,k}^{n}\,\delta x_{i+1}+\rho_{i+1,j,k}^{n}\,\delta x_{i})}$$
$$+g_x-\frac{\mathrm{FUX}_{i,j,k}^{n}+\mathrm{FUY}_{i,j,k}^{n}+\mathrm{FUZ}_{i,j,k}^{n}}{\mathrm{VFMX}_{i,j,k}} \quad (5)$$

Mixture energy equation

$$\frac{\rho_{i,j,k}^{n+1}I_{i,j,k}^{n+1}-\rho_{i,j,k}^{n}I_{i,j,k}^{n}}{\delta t^{n+1}}$$
$$=\frac{1}{\mathrm{VOL}_{i,j,k}}\left[S_{e_{i,j,k}}^{n+1}-\mathrm{FRIX}_{i,j,k}^{n}+\mathrm{FRIX}_{i-1,j,k}^{n}-\mathrm{FRIY}_{i,j,k}^{n}\right.$$
$$\left.+\mathrm{FRIY}_{i,j-1,k}^{n}-\mathrm{FRIZ}_{i,j,k}^{n}+\mathrm{FRIZ}_{i,j,k-1}^{n}\right]$$
$$-p^{n+1}\bar{\nabla}\cdot\bar{u}^{n+1}-\Gamma I_{\mathrm{stm}}+h_{\mathrm{NC}}A\,\Delta T. \quad (6)$$

The y and z components of the mixture momentum equations have similar forms. The terms FRAX and FRIX represent flows of air mass and mixture internal energy, respectively, across faces oriented perpendicular to the x axis. These are approximated by the usual weighted upstream/centered finite-difference approximations for a non-uniform mesh. [12] The terms ΓI_{STM} and $h_{\mathrm{NC}} A \Delta T$ represent energy changes due to condensation and wall heat transfer, respectively. In CAP, these forms are treated by extremely simple models. Their precise form is unimportant for an understanding of the basic solution method.

The continuum equation solution is based on the well known ICE [13] technique for compressible single phase flow. Selection of spatial and temporal differencing approximations (e.g., the use of advanced time pressures in Eq. (5) and advanced time velocities in the divergence term in Eq. (6)) has evolved through experience over a period of many years. The essence of the ICE technique is to provide a stable solution method for both high and low speed, incompressible flows.

The blockage of areas and volumes are implemented in a manner to simplify the mass and energy conservation equations. Since the flows of mass and energy are evaluated at mesh cell faces, we located areas there. Volumes are located at cell centers. Therefore, for example, the full expression for the air mass flow through the right hand face of cell i, j, k is given by

$$\mathrm{FRAX}^n_{i,j,k} = A^x_{i,j,k} u^{n+1}_{i,j,k} \left[\frac{(1+\alpha_x)\,\delta x_{i+1} \rho^n_{a_{i,j,k}} + (1-\alpha_x)\,\delta x_i \rho^n_{a_{i+1,j,k}}}{(1+\alpha_x)\,\delta x_{i+1} + (1-\alpha_x)\,\delta x_i} \right]$$

where

$$\alpha_x = \alpha\ \mathrm{SIGN}(u^n_{i,j,k}),$$

$A^x_{i,j,k}$ is the blocked flow area on that cell face and α is the spatial difference weighting factor. ($\alpha = 1.0$ for donor cell differencing and $\alpha = 0.0$ for centered differencing.) Figure 2A shows the mass cell and mass flows. Areas are located at the cell faces, that is, where the flows between cells are required. The volume is defined for this mass control volume (cell).

Next, consider the x-momentum equation. The non-conservative finite-difference equation (5) applies at the point $u_{i,j,k}$ as indicated in Fig. 2B. We must construct finite-difference approximations to the term

$$\frac{A_x}{\mathrm{VOL}} u \frac{\partial u}{\partial x} + \frac{A_y}{\mathrm{VOL}} v \frac{\partial u}{\partial y} + \frac{A_z}{\mathrm{VOL}} w \frac{\partial u}{\partial z}$$

which is represented by the notation [FUX + FUY + FUZ]/VFMX in Eq. (5). Unfortunately, the blockage fractions for A_y, A_z, and VOL are *not* defined at the same location as $u_{i,j,k}$. It is therefore necessary to reconstruct the flow blockages away from points where they are specified. We have chosen to visualize the blockage

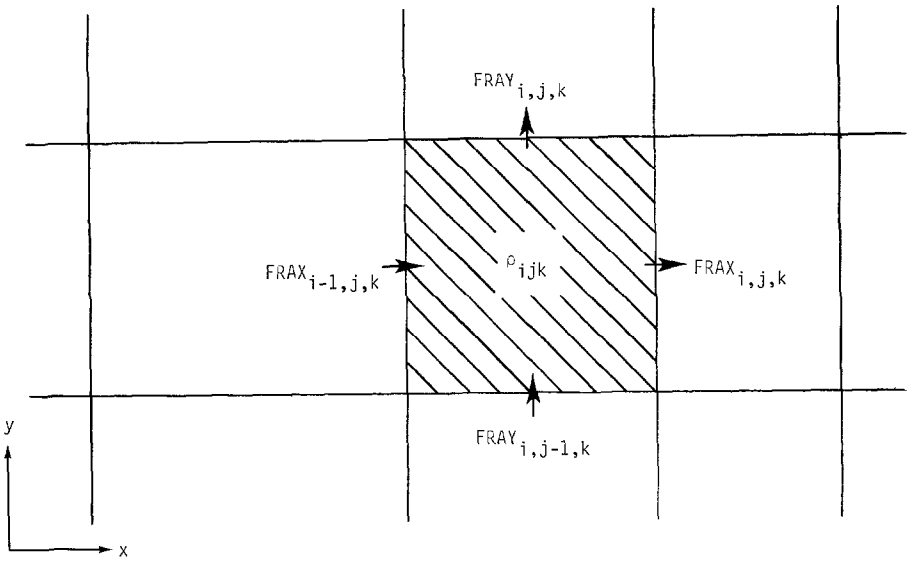

FIG. 2A. Mass cell and associated mass flows.

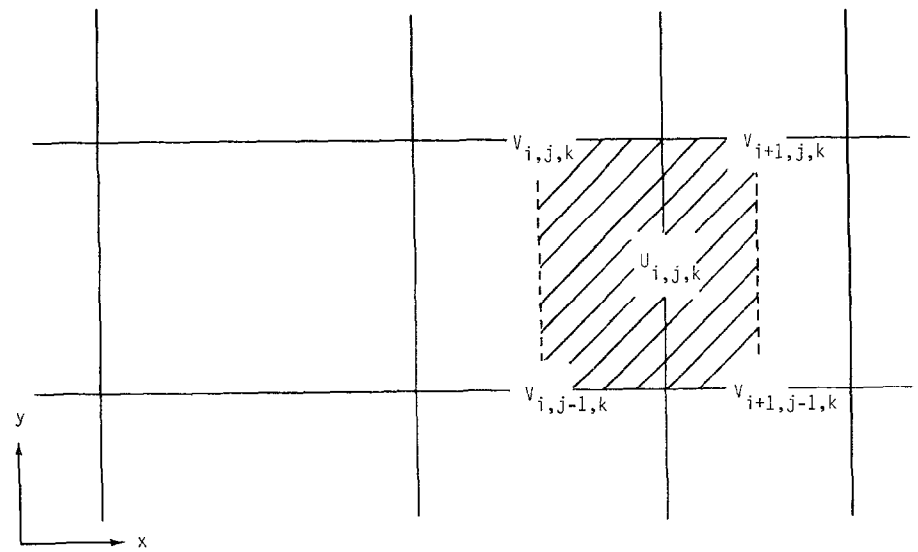

FIG. 2B. *U*-Momentum cell and *V*-velocities for $VFAV_{i,j,k}$.

as continuous, in conformance with our coarse computing mesh. We therefore interpolate to find the values associated with VOL and vA_y, as,

$$\mathrm{VFMX}_{i,j,k} = \frac{\mathrm{VOL}_{i,j,k}\,\delta x_{i+1} + \mathrm{VOL}_{i+1,j,k}\,\delta x_i}{\delta x_i + \delta x_{i+1}}$$

and

$$\mathrm{VFAV}^n_{i,j,k} = \frac{1}{2}\left[\frac{\delta x_i}{\delta x_i + \delta x_{i+1}}\left(A^y_{i+1,j,k}v^n_{i+1,j,k} + A^y_{i+1,j-1,k}v^n_{i+1,j-1,k}\right)\right.$$
$$\left. + \frac{\delta x_{i+1}}{\delta x_i + \delta x_{i+1}}\left(A^y_{i,j,k}v^n_{i,j,k} + A^y_{i,j-1,k}v^n_{i,j-1,k}\right)\right]$$

respectively. The finite-difference approximation for the term, for example, then becomes,

$$\frac{\mathrm{FUY}^n_{i,j,k}}{\mathrm{VFMX}_{i,j,k}} = \frac{\mathrm{VFAV}^n_{i,j,k}}{\mathrm{VFMX}_{i,j,k}}$$
$$\times\left[\frac{(1-\alpha_y)(\delta y_{j-1} + \delta y_j)\,\mathrm{DUDYP}^n_{i,j,k} + (1+a_y)(\delta y_j + \delta y_{j+1})\,\mathrm{DUDYM}^n_{i,j,k}}{(1-\alpha_y)(\delta y_{j-1} + \delta y_j) + (1+\alpha_y)(\delta y_j + \delta y_{j+1})}\right]$$

where

$$\mathrm{DUDYP}^n_{i,j,k} = \frac{u^n_{i,j+1,k} - u^n_{i.j.k}}{1/2(\delta y_j + \delta y_{j+1})}$$

$$\mathrm{DUDYM}^n_{i,j,k} = \frac{u^n_{i,j,k} - u^n_{i,j-1,k}}{1/2(\delta y_{j-1} + \delta y_j)}$$

and

$$\alpha_y = \alpha\ \mathrm{SIGN}(\mathrm{VFAV}^n_{i,j,k}).$$

III. Solution Algorithm and Particle Transport

Because the total density, ρ, occurs in the mixture-momentum and internal-energy equations, the above equations are incomplete as stated. They are completed by noting that

$$\rho_{i,j,k} = \rho_{a_{i,j,k}} + \rho_{h_{i,j,k}} + \rho_{s_{i,j,k}}$$

where $\rho_{h_{i,j,k}}$ and $\rho_{s_{i,j,k}}$ are the cell hydrogen and steam densities, respectively. These are evaluated from the positions and mass of the discrete particles. Therefore, the solution of the particle transport equations and the continuum equations must be intimately coupled.

The solution algorithm used in CAP is based on the ICE [13] technique. The time levels chosen in Eqs. (4)–(6) simplify inclusion of discrete particle transport. The solution algorithm proceeds in four steps: explicit velocity estimation, pressure iteration and final velocity update, particle transport, and mass and energy update.

The momentum equation in each direction is solved in the first step by approximating the pressure gradient explicitly. This explicit approximation uncouples the momentum equations from one another, which allows each to be integrated independently.

Solution for advanced time pressures during the second step is accompanied by altering the explicit velocity estimates to account for the effects of changes in pressure. This modification of the velocities stabilizes the solution, permitting substitution of the less restrictive material Courant condition for the classical condition based on combined material and sound speed. The pressure distribution is determined by requiring the equality of the equation of state density and the cell density modified by (Lagrangian) compression or expansion. Since this compression or expansion depends on the velocities, the result is a system of coupled, non-linear equations for the pressure. These are solved by CAP using either a point or line overrelaxation method.

Only explicit values of the cell densities are used in the first two steps. Advanced values appear, however, in the mixture energy equation. We, therefore, now turn to the transport of hydrogen and steam.

Particles are introduced into the system as initial conditions or by time-dependent sources. At its creation, a particle is assigned a position, a type (i.e., steam or hydrogen), and a mass. The velocity of each particle is the sum of a mean velocity (linearly interpolated to the particle position from the mean velocity field) and a random turbulent velocity. The basic idea is to consider the particle as a point source that diffuses for a time Δt. The density of this "Gaussian diffusion cloud" is then used as a probability density for where the original particle is likely to move. A random number generator selects the location actually used within the distribution. To estimate the size of the Gaussian cloud, it is necessary to have a local value for the turbulent diffusion coefficient. In CAP we use either a constant turbulent diffusion or one evaluated in terms of the local velocity gradients and a characteristic turbulent length scale (an input number to the code).

The particle transport algorithm considers each space coordinate separately; first y, then x, followed by z (this order is dictated by computational convenience in cylindrical coordinates). The velocity component is interpolated from cell edge values. The distance traveled is calculated by multiplying the velocity by the time-step size, δt. If the resulting new position is within the starting cell, its value is final. If a cell boundary is crossed, the probability of reflection is equated to the blocked area fraction on the face and the reflection is assumed to be specular.

Usually, the time increment for particles is the same as that for the continuum equations. In certain cases, however, where the continuum flow is steady, or nearly steady, the particles could be repeatedly advanced with a separate time step.

Once all particle locations have been fully updated in this manner, the steam and hydrogen densities can be readily calculated from particle positions. Loss of particles at sinks or through condensation of steam is accounted for during the solution of the mixture energy equation.

The air mass equation (4) is solved next. The first step is calculation of the air mass flows through cell faces. The mixture energy flows needed for the solution of Eq. (6) are evaluated simulateneously. Complete solution of the mixture energy equation requires evaluation of sinks, wall and bulk condensation, and heat transfer, since these modify the cell energy content and the cell density. The effects of these processes are calculated on a cell basis to permit evaluation of the cell mixture internal energy. Condensation and sinks must also be reflected in the particle field. This is accomplished by reducing the mass of every steam or hydrogen particle in a cell by a uniform fraction. A minimum particle mass is enforced by a "Russian Roulette" technique that maintains the correct mass on the average. That is, if the mass of any particle falls below a user-defined minimum, the particle is either eliminated or its mass is set to five times the minimum. This is done randomly so that the average mass is conserved.

IV. Sample Calculations

To exhibit the accuracy of results calculated by CAP in compressible flow situations, we shall compare them with the analytic solution of a one-dimensional shock tube problem. Comparisons with data taken at Battelle–Frankfurt [14] show CAP's capabilities and limitations in essentially-incompressible buoyancy-driven flows. Comparisons with other experiments (including one that is fully three-dimensional) can be found in Ref. [15].

The shock tube calculation models a closed tube with an initial discontinuity in pressure at its midpoint. The analytic solution [16] consists of shock and rarefaction waves and a contact surface traveling away from the initial discontinuity. The initial pressure discontinuity has a pressure ratio of 3 : 1, which is similar to the pressure pulse observed during the Three Mile Island incident. The tube is modeled by a one-dimensional sequence of 65 mesh cells. The initial pressure discontinuity is located at the right hand edge of cell 25. To permit tracking of the contact surface, particles were initially placed throughout the high pressure half of the tube, representing 10% of the initial mass in that region. (For this calculation hydrogen properties were modified to simulate air, simplifying the analytic solution.) No turbulence effects were included in either the analytic or calculated solutions.

Figures 3–5 compare the analytic and computed pressure, density, and temperature distributions after 5 milliseconds. Considering the coarseness of the mesh used for

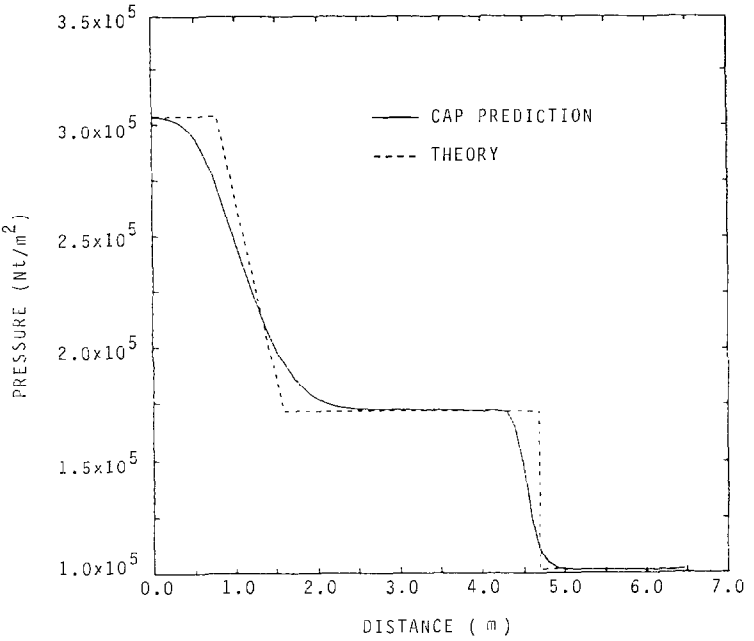

FIG. 3. Pressure distribution at 5 msec in a 3 : 1 shock tube calculation.

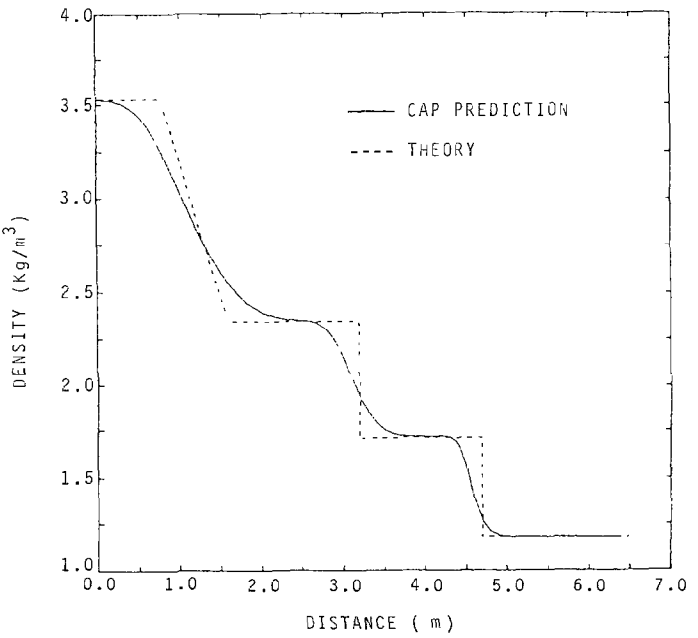

FIG. 4. Density distribution at 5 msec in a 3 : 1 shock tube calculation.

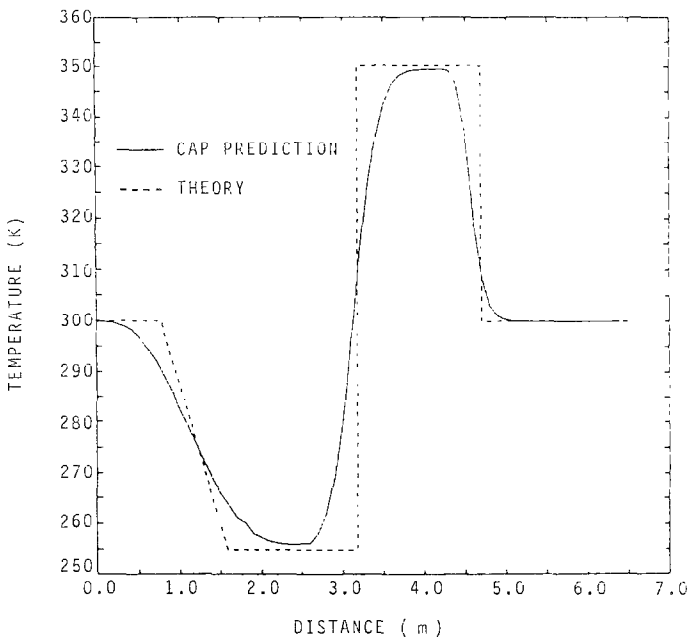

FIG. 5. Temperature distribution at 5-msec in a 3 : 1 shock tube calculation.

this calculation, the calculated pressure, density, and temperature plateaus agree well with the analytic solutions, as do the locations of the rarefaction wave, contact surface and shock. The transitions between regions of the solution are expanded by numerical diffusion in the calculation. (The analytic solution in the rarefaction region is approximated as linear in these comparisons.)

In contrast, the partial pressure of hydrogen (air) particles is compared with the analytic result in Fig. 6. There is *no* expansion of the contact surface in this figure. the drop to zero takes place over the length of a single cell. There are, however, some fluctuations evident that arise from the discrete nature of the particles.

The mixing of hydrogen and air in reactor containment buildings has been investigated through a sequence of tests at Battelle Memorial Institute, Frankfurt, West Germany [14]. Two of the simpler tests have been analyzed using CAP to confirm its ability to predict buoyantly driven flows.

Both tests were performed in the cylindrical, two-compartment experimental facility depicted in Fig. 7. Hydrogen was slowly introduced into the system through a permeable bladder at the bottom of the test compartment. The buoyant force induced a mean flow up along the compartment center line, out to the wall and down along the outer wall. In test 2 there were no temperature variations between the compartments and the resulting flow carried hydrogen into both compartments in spite of the flow area restriction between them. Test 6 maintained a higher temperature in the upper compartment, which effectively prevented hydrogen from entering that compartment.

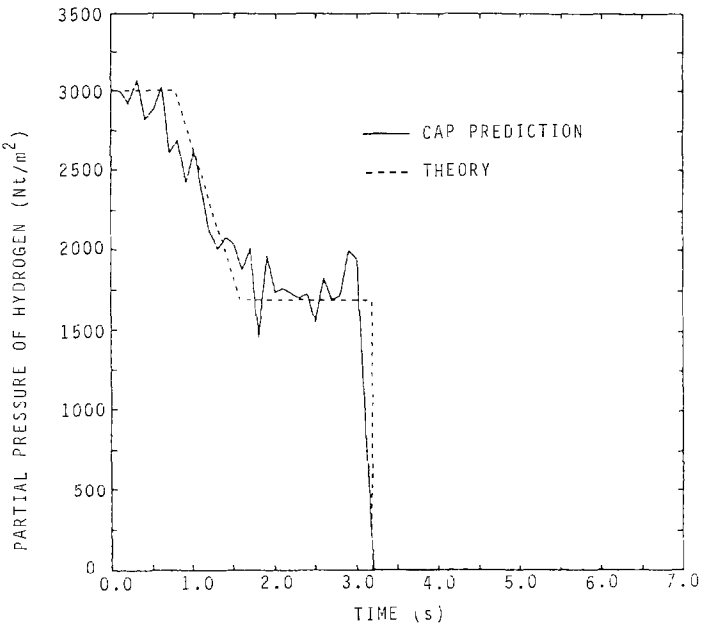

FIG. 6. Representation of contact surface by hydrogen particles at 5 msec in a 3 : 1 shock tube calculation.

The CAP simulations of these tests were performed in two-dimensional, cylindrically-symmetric geometry. The two compartments were modeled with a central window permitting flow between them. The mesh shown in Fig. 8 was used in both calculations. Note that the indentation within the lower compartment has been modeled as a partial flow-area restriction in this coarse mesh.

The calculated velocity fields for tests 2 and 6 are shown in Figs. 9A and B, respectively. (Different periods of time were simulated for the two tests, but both calculations quickly reached quasi-steady velocity distributions.) Test 2 results show the developed full-system eddy, while test 6 results display separated eddies in the upper and lower compartments. (We suspect that the upper eddy is an artifice of the finite-difference approximation of flux terms in the momentum equation. A different formulation of the appropriate terms is under development to address this difficulty.)

To permit monitoring of local concentrations of particles, CAP provides a special output mechanism called a particle detector. These detectors can be located at any point in the system and occupy user specified volumes. Figures 10 and 11 compare the readings from two CAP particle detectors with measured data for test 2. The measurements were taken on the centerline of the system at the center and top, as shown in Fig. 7 (measurement points 83 and 88). Notice the presence of strong fluctuations in the calculated result in these figures. These fluctuations are a direct result of the discrete representation of hydrogen in CAP. Because a limited number of particles is dictated by cost considerations (646 particles were in the system at the

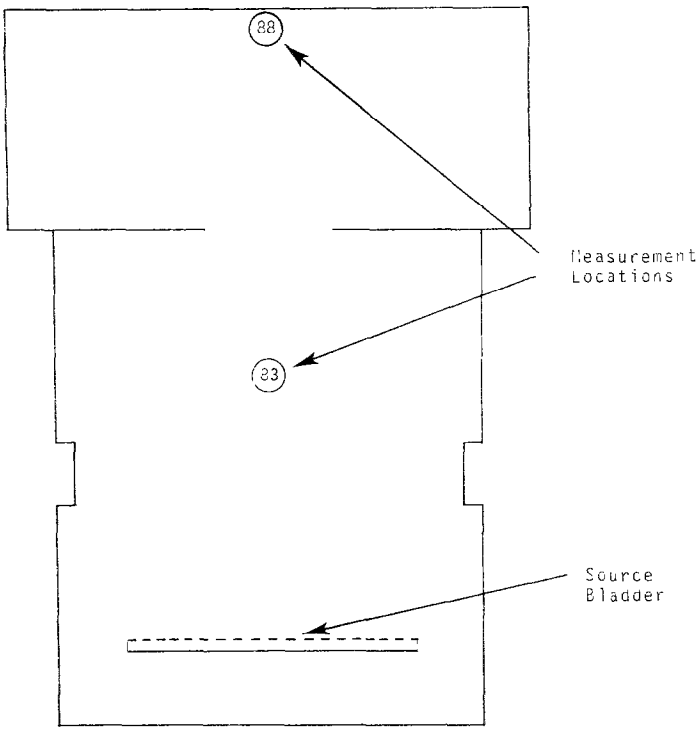

FIG. 7. Battelle–Frankfurt experimental configuration for tests 2 and 6.

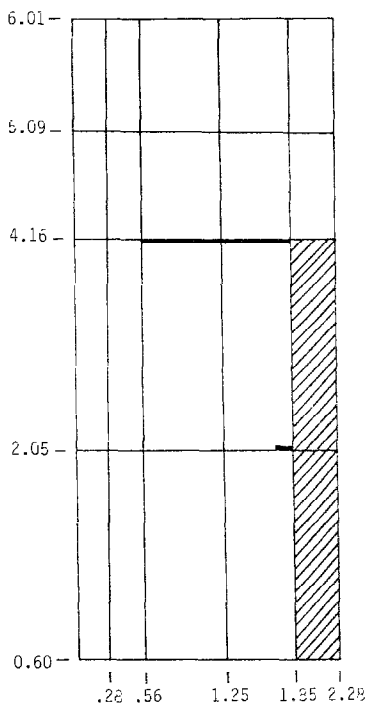

FIG. 8. CAP noding for Battelle–Frankfurt calculations (dimensions in meters).

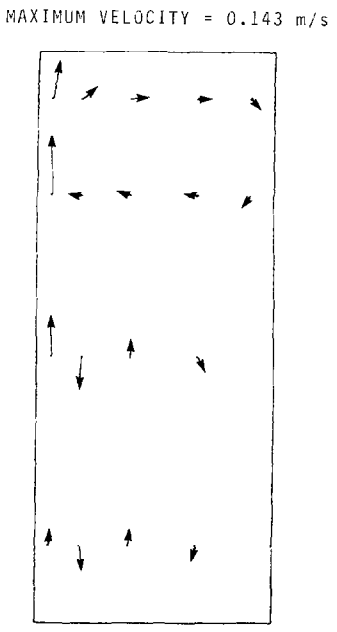

FIG. 9A. Battelle–Frankfurt test 2 velocity vectors at 1000 seconds.

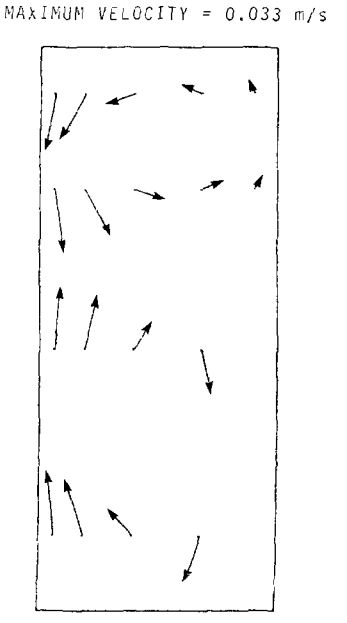

FIG. 9B. Battelle–Frankfurt test 6 velocity vectors at 2833 seconds.

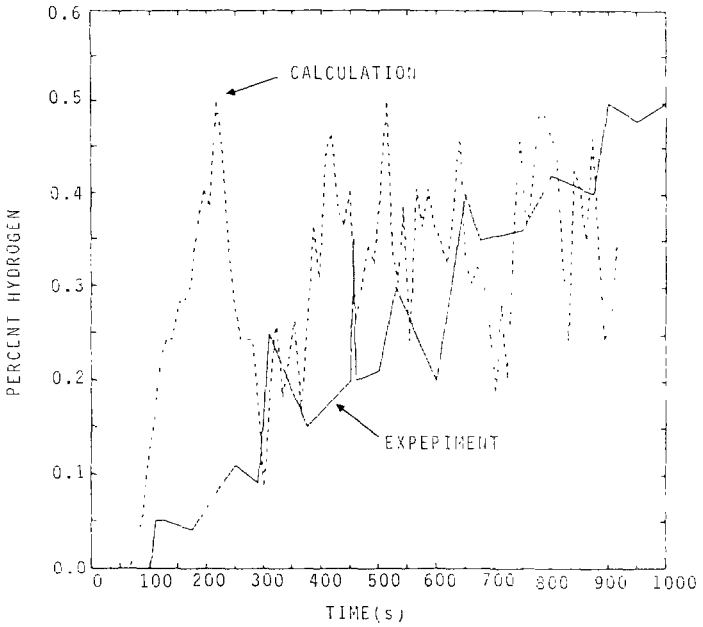

FIG. 10. Calculated and measured percent hydrogen at detector 83 for test 2.

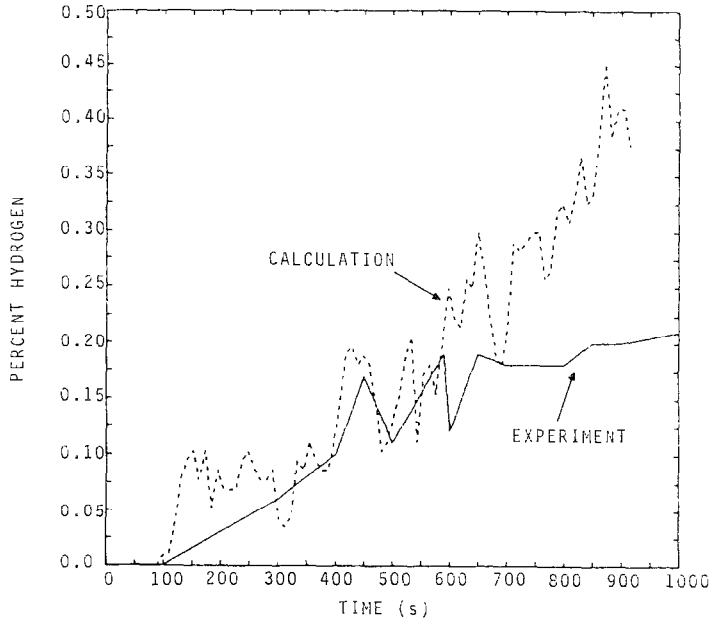

FIG. 11. Calculated and measured percent hydrogen at detector 88 for test 2.

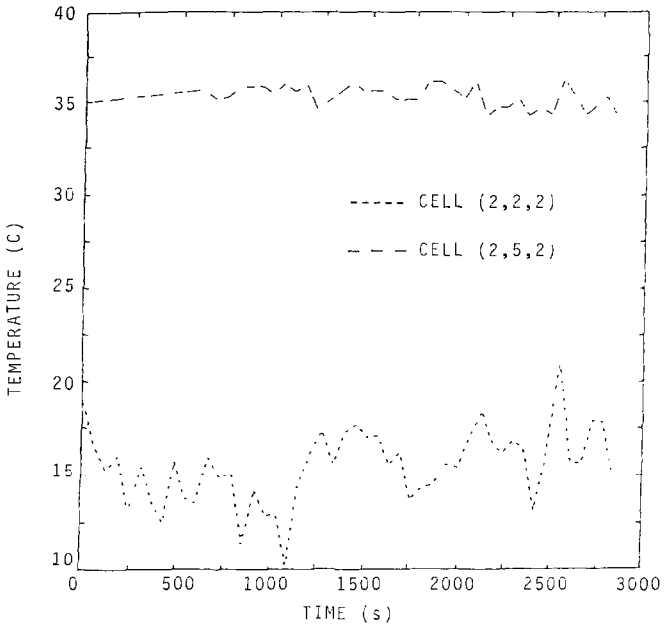

FIG. 12. Calculated temperature histories above and below the baffle for test 6.

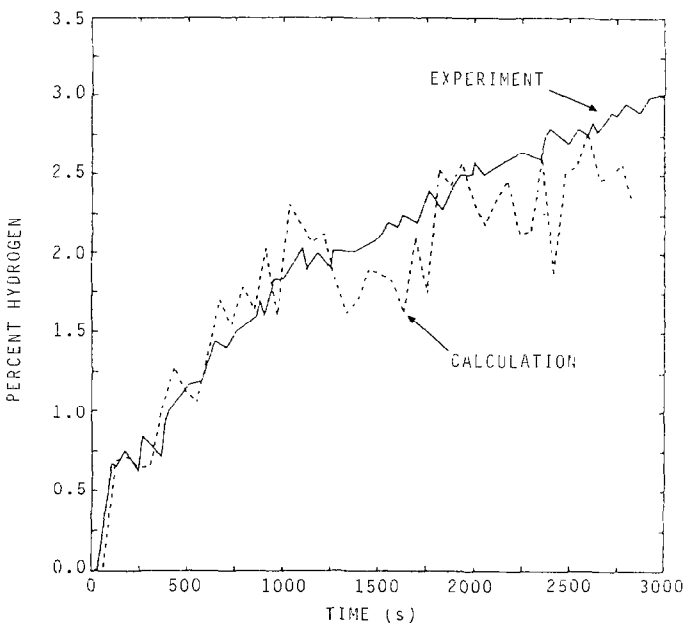

FIG. 13. Calculated and measured percent hydrogen at detector 83 for test 6.

end of this calculation), these fluctuations are considerable. Another result of the discrete particle formulation is visible in Fig. 12, which shows calculated temperatures in the upper and lower compartments for test 6. Again, the fluctuations are due to the discrete representation, magnified in this case by the energy convection algorithm. Since the mixture energy is transported on a continuum basis, the discrete mass transport results in temperature fluctuations. In calculations that contain steam as well as hydrogen particles, large fluctuations may cause serious problems by inducing condensation [15].

It is relatively clear from these results that a significant improvement could probably be made to the CAP technique by transporting energy as well as mass with the particles. Unfortunately, funding and time constraints prevented any investigation of such improvements. Of course, fluctuations can also be reduced by increasing the number of particles at the cost of increased computational effort and storage.

If one focuses on the mean behavior, mentally filtering the fluctuations, we see reasonable average agreement between the calculation and experiment, the concentration of hydrogen is nearly uniform in the system.

In contrast, there is distinct non-uniformity between the upper and lower compartments in test 6, as shown in Figs. 13 and 14. (Note the change in concentration scale in these figures.) CAP has reproduced both the gross convection patterns generated by buoyancy of hydrogen and the influence of a temperature stratification, which provides a counterbalancing buoyancy force to that of hydrogen.

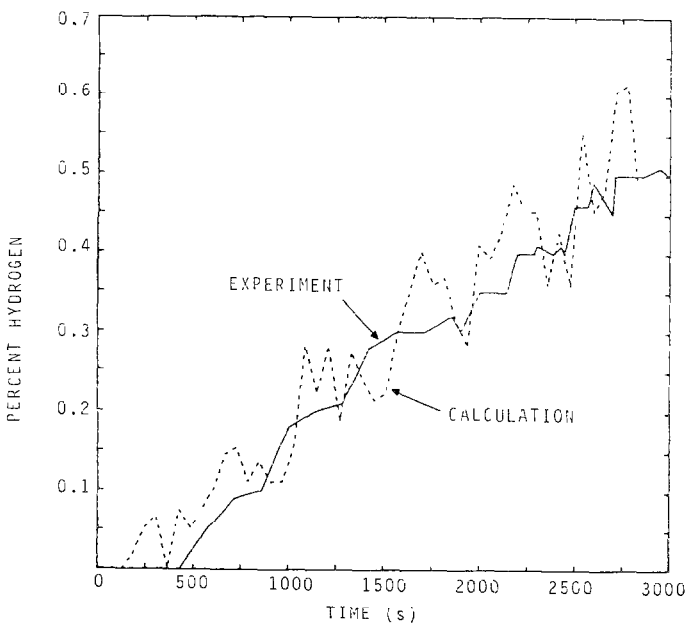

FIG. 14. Calculated and measured percent hydrogen at detector 88 for test 6.

Test 6 simulation (to 2833 seconds) included 2160 particles and required 560 CPU seconds on a CDC-750 computer, compared with 72 CPU seconds for test 2. (A CDC-750 is approximately half the speed of a CDC-7600.)

V. Conclusion

The flow of contaminants has been modeled by a combination of discrete, Lagrangian-like particles representing the contaminants and a continuum, Eulerian representation of the background flow. This scheme has the advantage of eliminating numerical diffusion of the contaminant because it is tracked in a Lagrangian manner, while permitting a coarse mesh for the resolution of the flow, thus achieving low computational cost. Use of flow area and volume blockages enhances our ability to model complex geometric situations with few computational volumes.

Applications of a specific implementation of the algorithm (CAP) to two situations has been displayed. CAP was developed to evaluate the mixing of hydrogen and air in nuclear reactor containment buildings. Comparisons with analytic results for a shock tube problem and data for a hydrogen mixing experiment show generally good agreement, although fluctuations due to the statistical nature of the discrete particles must be expected.

References

1. C. W. Hirt and J. L. Cook, *J. Comput. Phys.* **10** (1972), 324.
2. C. W. Hirt, J. M. Sicilian, and R. P. Harper, "SOLA-3D/FSI: A Solution Algorithm for Transient Three-Dimensional Flows," Flow Science, Inc. Report FSI-83-00-3 , July 1983.
3. A. A. Amsden, "The Particle-In-Cell Method for the Calculation of the Dynamics of Compressible Fluids," Los Alamos Scientific Laboratory Report LA-3466, June 1966.
4. W. C. Rivard and M. D. Torrey, "*K*-FIX: A Computer Program for Transient Two-Dimensional, Two-Fluid Flow," Los Alamos Scientific Laboratory Report LA-NUREG-6623, April 1977.
5. "TRAC-PD2: An Advanced Best-Estimate Computer Program for Pressurized Water Reactor Loss-of-Coolant Accident Analysis," Los Alamos Scientific Laboratory Report LA-8709-MS, April 1981.
6. M. J. Thurgood, "COBRA-TF: A Thermal Hydraulics Code for Transient Analysis of Nuclear Reactor Components, Vol. IV-B, User's Manual for Containment Analysis (COBRA-NC) and Vol. VII Assessment Manual for Containment Applications," Battelle, Pacific Northwest Laboratories, NUREG/CR-3269, October 1983.
7. J. O. Henrie and A. K. Postma, "Analysis of the Three Mile Island (TMI-2) Hydrogen Burn," Second International Topical Meeting on Nuclear Reactor Thermal Hydraulics, Sponsored by the American Nuclear Society, American Society of Mechanical Engineers, and the American Institute of Chemical Engineers, Santa Barbara, CA, January 1983.
8. USNRC, "Interim Requirements Related to Hydrogen Control," Federal Register, December 23, 1981 (46 FR 62281).
9. J. R. Travis, "HMS: A Model for Hydrogen Migration Studies in LWR Containments," Los Alamos National Laboratory Report LA-82-2701, Second International Workshop of the Impact of Hydrogen on Water Reactor Safety, Albuquerque, NM, October 1982.

10. L. L. EYLER AND D. S. TRENT, "TEMPEST: Computer Code Model and Results of HEDL Hydrogen Mixing Tests, Standard Problems A and B," Battelle, Pacific Northwest Laboratories, Hydrogen Mixing Standard Problems A and B Review Meeting, Electric Power Research Institute, July 1982.
11. M. J. THURGOOD, "Application of COBRA-NC to Hydrogen Transport," Battelle, Pacific Northwest Laboratories, Second International Workshop on the Impact of Hydrogen on Water Reactor Safety, Albuquerque, NM, October 1982.
12. B. D. NICHOLS, C. W. HIRT, AND R. S. HOTCHKISS, "SOLA-VOF: A Solution Algorithm for Transient Fluid Flow with Multiple Free Boundaries," Los Alamos National Laboratory Report LA-8355, 1980.
13. F. H. HARLOW AND A. A. AMSDEN, *J. Comput. Phys.* **8** (1971).
14. G. LANGER, R. JENIOR, AND H. G. WENDLANDT, "Experimental Investigation of the Hydrogen Distribution in the Containment of a Light Water Reactor Following a Coolant Loss Accident," Battelle Institut e.V. Frankfurt Report BF-F-63, 363-3 (NRC Translation 801), May 1979.
15. J. M. SICILIAN AND C. W. HIRT, "Simulations of Hydrogen Mixing Using the Containment Atmospheric Prediction Code," Electric Power Research Institute Report, NSAC-59, October 1983.
16. F. H. HARLOW AND A. A. AMSDEN, "Fluid Dynamics," Los Alamos Scientific Laboratory Report LA-4700, June 1971.